Click Here for Full Article

Lifetime and longitudinal variability of equatorial Kelvin waves around the tropical tropopause region

Junko Suzuki,[1] Masato Shiotani,[2] and Noriyuki Nishi[3]

[1] Using the European Centre for Medium-Range Weather Forecasts 40 year reanalysis data for zonal wind fields, we investigated the characteristic variability and mean lifecycle of Kelvin waves around the tropical tropopause layer and upper troposphere. The distributions of Kelvin wave activity, mean squared amplitude, and number of passing cases closely resemble each other. Kelvin wave disappearance locations relative to appearance longitudes were examined at 200 and 100 hPa. At 200 hPa Kelvin waves mostly appear in the western hemisphere. At 100 hPa the highest-frequency region is centered in the eastern hemisphere. On average, eastward propagation extending over ~80° in longitude occurs at both levels examined. Mean lifecycle and its relation to background conditions were analyzed with a composite method. In a typical example at 200 hPa, Kelvin waves appear over the Indian Ocean and western Pacific, propagate eastward through westerly basic winds, decrease over South America, and then accelerate eastward. Their vertical structure has divergence in the upper and middle troposphere and weak convergence in the lower troposphere, tilting eastward with height. At 100 hPa, Kelvin waves typically propagate eastward in easterly basic winds and then decrease over a region between the Indian Ocean and western Pacific Ocean. Kelvin wave signals continuing over South America suggest that some waves first recognized in the western hemisphere at 200 hPa propagate upward and eastward near South America, reaching 100 hPa in the eastern hemisphere. Temperature anomalies in both hemispheres show the boomerang-like vertical structure while associated with eastward-propagating convections, which suggests at least some waves are convectively coupled.

1. Introduction

[2] Many studies of the tropical atmosphere have provided detailed analyses of waves and oscillations. In particular, Kelvin waves in the tropical tropopause layer (TTL) have been examined from the viewpoint of stratosphere-troposphere exchange (STE) in the tropics, because Kelvin waves are one of the largest-amplitude disturbances in the temperature field around the TTL [*Suzuki and Shiotani*, 2008, hereafter SS08]. The space-time characteristics of Kelvin waves around the tropical tropopause were described by *Tsuda et al.* [1994] using radiosonde data at Indonesia. Thereafter, it has been obvious that Kelvin waves around the TTL play important roles in the dehydrating mechanisms in the lower stratosphere because of differences in water vapor content observed between the upward and downward

displacement phase of Kelvin waves [*Fujiwara et al.*, 2001] and occurrence of cirrus clouds frequently observed in the upper troposphere and tropopause [e.g., *Winker and Trepte*, 1998; *Peter et al.*, 2003] which is related to the cold phase of the Kelvin waves [*Boehm and Verlinde*, 2000; *Immler et al.*, 2008]. From the viewpoint of chemical species across the TTL, an episode of stratospheric ozone transport into the upper troposphere associated with a breaking Kelvin wave [*Fujiwara et al.*, 1998] and the correlation between temperature and ozone variation in the upper troposphere at Nairobi in June–August owing to Kelvin wave passage from the upper troposphere to the tropopause [*Takashima and Shiotani*, 2007] were observed using the ozonesonde and radiosonde data.

[3] Many previous studies have been found that Kelvin waves are one of the important westerly momentum transports responsible for driving the quasi-biennial oscillation in the stratosphere [e.g., *Baldwin et al.*, 2001]. Kelvin waves should be triggered mostly by diabatic heating associated with organized deep convection [e.g., *Holton*, 1972; *Salby and Garcia*, 1987]. Recently, *Ryu et al.* [2008] found that a Kelvin wave could respond to convective heating in the Madden-Julian Oscillation (MJO) system and vertically

[1]Research Institute for Global Change, Japan Agency for Marine-Earth Science and Technology, Yokosuka, Japan.
[2]Research Institute for Sustainable Humanosphere, Kyoto University, Uji, Japan.
[3]Graduate School of Science, Kyoto University, Kyoto, Japan.

propagate at a higher phase speed through the TTL than the MJO's. In the troposphere, tropical convective eastward disturbance with the Kelvin wave structure in dynamical fields has often been assumed as a convectively coupled Kelvin waves system [e.g., *Takayabu*, 1994; *Wheeler and Kiladis*, 1999]. *Wheeler et al.* [2000] showed vertical structure of the convectively coupled Kelvin wave, and referred to its possible influence on the temperature and zonal wind fields up to the tropical tropopause and lower stratosphere. In all likelihood, the variability of Kelvin wave activity in the TTL can be attributed to the basic wind conditions and energy source scale.

[4] Of these two factors, the basic zonal wind around the TTL was likely to adjust amplitudes of waves propagating upward as found in a companion paper (SS08). We demonstrated that the space-time variability of Kelvin waves in the TTL using dynamical data from the European Centre for Medium-Range Weather Forecasts (ECMWF) 40 year reanalysis (ERA-40) widely used for approximate observational studies on the tropical atmosphere, including the troposphere and stratosphere. At two adjoining levels of the ERA-40 data around the TTL, 100 and 150 hPa, the wave activity showed the same seasonality: Kelvin wave activity was vigorous in January–March and June–August; also, the waves had larger amplitudes in the TTL than in the troposphere. In contrast, there was a clear difference in the maximum longitude; at 100 hPa it was located in the eastern hemisphere, but at 150 hPa and below it was located in the western hemisphere. As the climatological background zonal wind in the upper troposphere was easterly in the eastern hemisphere and westerly in the western hemisphere, it seemed that the difference in Kelvin wave activities at 100 and 150 hPa was closely related to the basic wind affecting Kelvin wave propagation and dissipation. However, some questions remain, for instance, whether the large Kelvin wave activity region was caused by a few large-amplitude waves or many small-amplitude waves.

[5] Using the ERA-40 data, *Nishi et al.* [2007] showed that cases with a rapid increase in the zonal wind occurred in the eastern hemisphere at 100 hPa, because the Kelvin waves were amplified and nonlinearly distorted by the basic zonal wind. *Ryu et al.* [2008], using simulations data from a global primitive equation model, suggested that vertically propagating Kelvin waves reached maximum amplitude over the western Pacific around the TTL because of zonal variations in the basic zonal wind, regardless of the position of the imposed heating. However, not only the distribution of Kelvin wave amplitudes but also the energy source region producing each Kelvin wave remains obscure.

[6] The longitudinal variation in Kelvin wave activity was more remarkable than the seasonal variation in the results of SS08 using the ERA-40 data. Furthermore, *Alexander et al.* [2008] distinguished both longitudinal and monthly variability using temperature data of high vertical resolution around the TTL obtained from the Global Positioning System (GPS) radio occultation technique. Therefore, we investigate further to resolve the above questions in this paper from the view point of longitudinal variation using the Kelvin wave extraction method described in detail in section 2. This method makes it possible to find individual Kelvin waves passing through a region and their amplitudes. Here, Kelvin waves would contain

both convectively coupled waves and so-called free waves sufficiently distant from deep convections working as energy source. It would be difficult to separate both type of waves, because by seasons and regions Kelvin waves could have various vertical and horizontal structures including convections.

[7] In this paper, the data and methodology are described in section 2. In section 3.1, we present the results of the analysis for the extracted Kelvin waves around the TTL, which reveals several characteristics of variability, and we describe the composite structures and lifecycles in section 3.2. A summary is presented in section 4.

2. Data and Methodology

[8] As by SS08, to detect and investigate Kelvin waves in the dynamical fields, the ERA-40 global analysis data were obtained from the ECMWF for the period September 1957 to August 2002 on $2.5° \times 2.5°$ grids. Detailed descriptions of the ERA-40 data are available from *Uppala et al.* [2005]. The original data are available for every 6 h, but in this study we averaged on a daily basis. Zonal wind and temperature fields were used to analyze Kelvin waves on the basis of wave dynamical structure. There are 23 pressure levels from 1000 to 1 hPa; we focused mainly on the Kelvin waves found between the upper troposphere at 200 hPa ($\sim$12.0 km) and the tropopause region at 100 hPa ($\sim$16.6 km). Data up to 50 hPa are investigated for analyzing Kelvin waves. *Ern et al.* [2008] indicate that the Kelvin wave variabilities in temperature from ECMWF are good agreement with those from SABER satellite about the longitudinal distribution in the lower stratosphere. Daily outgoing longwave radiation (OLR) data from the NOAA polar-orbiting satellites is also available on $2.5° \times 2.5°$ grids over the period from January 1979 to August 2002; this was used as a proxy of convective activity.

[9] We begin by extracting the Kelvin wave signals by filtering the zonal wind for the specific region of the Kelvin wave wave number–frequency domain; this includes zonal wave numbers from 1 to 10, periods (frequencies) from 4 to 23 days (from 0.0435 to 0.250 d^{-1}), and equivalent depths (phase speeds) from 8 to 240 m (from 8.9 to 48.5 m s^{-1}). This domain is the same as that applied for Kelvin waves by SS08. Note that this region of wave number–frequency filtering extends to higher equivalent depths (up to 240 m) compared to that used for studying convectively coupled Kelvin waves by *Wheeler and Kiladis* [1999] which is up to 90 m. Hereafter, this reconstructed data set is called "the Kelvin wave data" for simplicity.

[10] Previous studies have investigated the vertical structure of Kelvin waves by focusing on the phase relation to the dynamical fields in the troposphere–lower stratosphere and to convective activity. They have suggested that the convective center is located longitudinally near the largest easterly wind anomaly at 100 hPa [e.g., *Wheeler et al.*, 2000; *Straub and Kiladis*, 2003]. Therefore, we choose to follow the Kelvin wave signals around the TTL using the easterly wind rather than the westerly. In addition, the easterly wind anomaly at 200 hPa is near zero on the center of convective longitude. To pick up isolated Kelvin wave events from the Kelvin wave data, we set the threshold as the easterly component with -1σ at each height (e.g.,
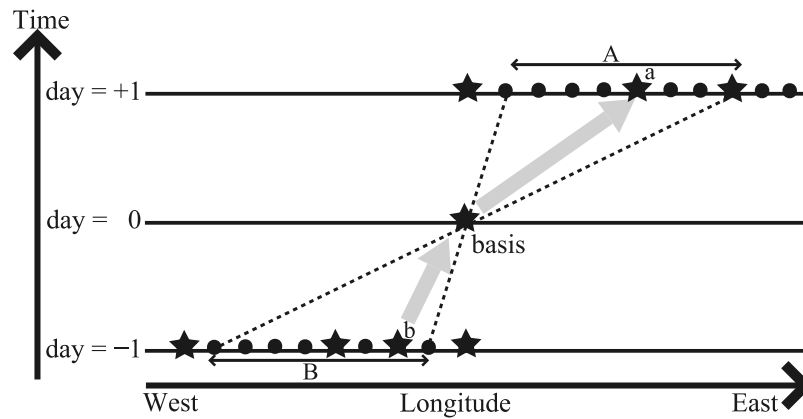
Figure 1. A schematic illustration of a longitude-time section of the selected Kelvin wave locus at a pressure level field. Stars (dots) show grid points above (below) the threshold as the easterly component with $-1\,\sigma$ at each pressure field. Arrow A (B) shows the possible arrival (return) longitudinal range from the "basis" grid point estimated from the phase speed defined by the Kelvin wave filter. The black stars a and b show the selected grids as the passage of the same Kelvin wave. Therefore, the gray arrows show the route of the selected Kelvin wave. See details in the text.

-2.87 m s^{-1} at 200 hPa; -2.98 m s^{-1} at 100 hPa). Here, 1σ means the largest standard deviation of all values calculated on each longitudinal grid point for 45 years, and the Kelvin wave easterly maxima are defined as the grid points with the largest value among the five neighboring grid points in the longitudinal and time directions.

[11] Figure 1 shows a longitude-time section explaining the Kelvin wave extraction method. Stars represent the easterly maxima of Kelvin waves and dots show grid points below the threshold. Arrow A (B) shows the horizontal range of possible arrival (return) from the basis point; two dotted slanting lines correspond to the maximum and minimum phase speeds already defined by the Kelvin wave filter. This limit to the phase speed avoids catching the point on a jump grid when we extract successive signals as a Kelvin wave. Stars of easterly maximum inside of A (B) are recognized as successive signals from the basis. If multiple stars of easterly maxima exist on the same day, the star longitudinally close to the basis is selected as the successive signal (e.g., stars a and b) to avoid choosing grid points belonging to the other waves.

[12] If the basis point does not have a successive signal on the previous (next) day, it is recognized as an appearance (disappearance) location. Note that the appearance (disappearance) point is where the Kelvin wave appears (disappears) at one pressure level; the Kelvin wave signal might also be found at proximate pressure levels. Also note that the appearance point does not mean the energy source region where the Kelvin wave is produced.

3. Results

3.1. Variability of Kelvin Waves

[13] Figure 2 shows longitude-time sections in 1990 for deep convections in OLR and Kelvin wave events in zonal wind at 200 hPa (Figure 2a) and 100 hPa (Figure 2b). This year is recognized as a normal year of the El Niño-Southern Oscillation (ENSO) cycle. Dynamical parameters are averaged over the equator between 5°S and 5°N to investigate the dynamical structures of Kelvin waves near the equator.

Whereas, the OLR data is averaged between 10°S and 10°N, because organized convection located away from the equator sometimes affects the dynamical fields over the equator [e.g., *Straub and Kiladis*, 2002].

[14] The black stars show the easterly wind maxima of Kelvin waves exceeding the easterly threshold corresponding to the stars in Figure 1. In Figure 2, the envelope lines including the easterly maxima show the passing regions at one pressure level for Kelvin waves propagating eastward. The easterly maxima of Kelvin waves are found throughout the year in all longitudes; the total number of extracted Kelvin waves is over 3000 for 45 years. We first focus on Figure 2a, the 200 hPa level, as an upper troposphere region near the beginning for Kelvin waves that could propagate to the tropopause region.

[15] The obvious feature is that many signals are distributed over the whole of the western hemisphere. Three convectively active regions appear: Africa (around 0°E–30°E), the Indian Ocean and the western Pacific (60°E–150°E), and South America (80°W–45°W). Many Kelvin waves originate at 200 hPa ("S" in Figure 2a) around the dateline near the eastern edge of the convective region in the western Pacific. Kelvin wave disappearance points from 200 hPa ("E" in Figure 2a) exist in the western hemisphere. Many waves leave their traces throughout about 120°, and furthermore some waves track halfway around the globe (e.g., the signal appearing first around 150°W in mid-August).

[16] In contrast, many appearance points at 100 hPa are located around the Greenwich meridian and in the eastern hemisphere (Figure 2b). Easterly maxima of Kelvin wave signals at 100 hPa frequently pass through the convective regions over Africa and between the Indian Ocean and the western Pacific. Hereafter, we use the easterly maximum as a Kelvin wave signal. For further details about the relations between Kelvin waves and convective activity, we will demonstrate on the basis of the composite lifecycles of Kelvin waves in section 3.2.

[17] Figure 3 shows comparable longitude-height cross sections for three Kelvin wave characteristics in zonal wind.
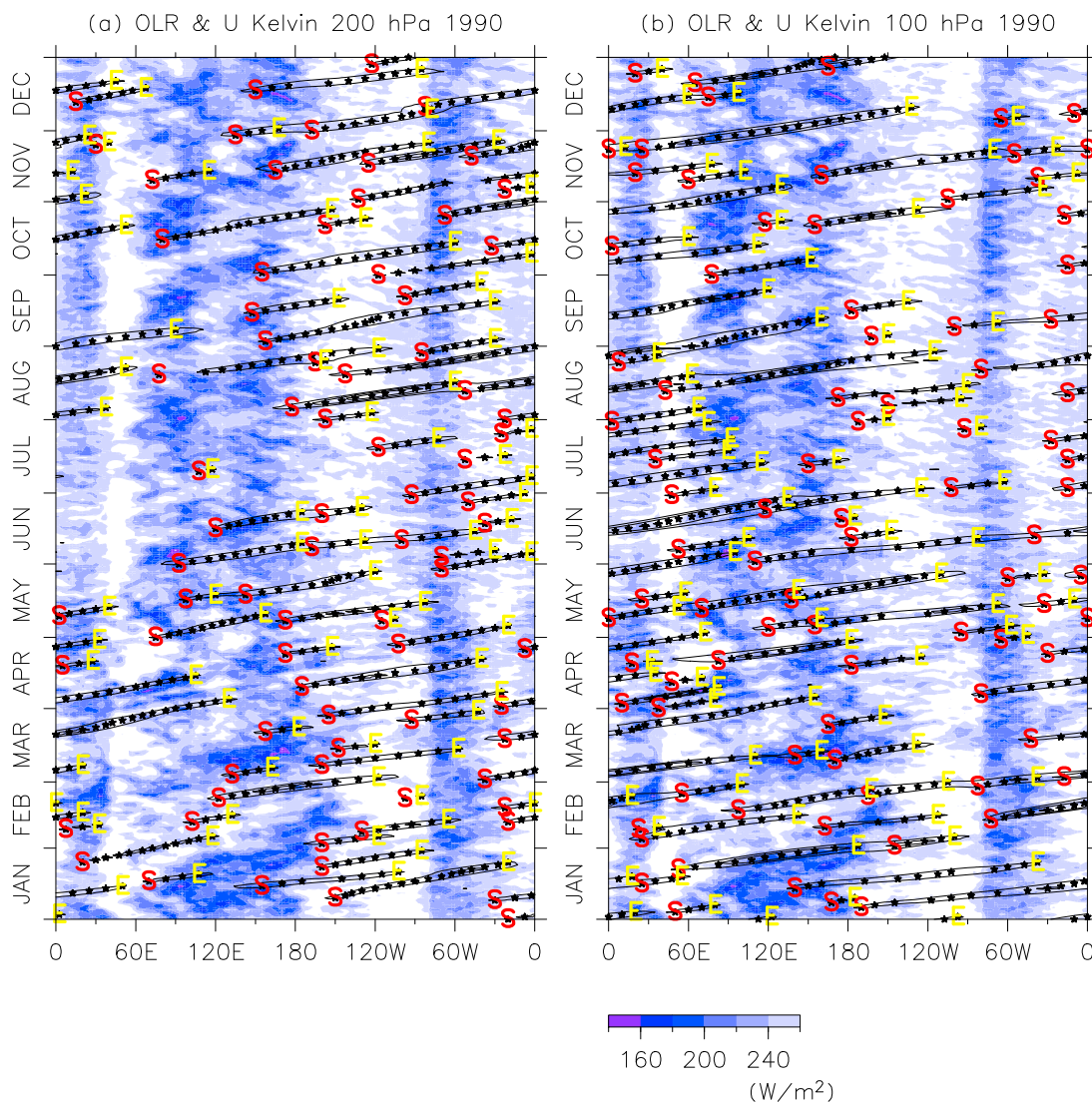
Figure 2. Longitude-time sections in 1990 of the outgoing longwave radiation (OLR) averaged over latitudes $10°S-10°N$ (colors) and the Kelvin wave signals for the zonal wind averaged over latitudes $5°S-5°N$ (contours) at (a) 200 hPa and (b) 100 hPa. Contour interval is 2.87 m s^{-1} in Figure 2a and 2.98 m s^{-1} in Figure 2b and indicates a value less than 0 m s^{-1} (the easterly wind anomaly). Contour interval corresponds to the threshold to pick up isolated Kelvin wave event (see detail in the text). The stars show the easterly maxima for the Kelvin wave signals. They correspond to the black stars in Figure 1. The letter S (E) represents the wave starting (ending) grid point at each pressure level.

Figure 3a is reproduced from *Suzuki and Shiotani* [2008, Figure 7a], in which the values show the annual mean of Kelvin wave activity defined as the squared amplitude. Longitudes of the maximum activity are quite different at each height. As seen in Figure 2, the active region is observed in the western hemisphere at 200 hPa, but in the eastern hemisphere it appears at 100 hPa. Because this parameter can include activity induced by waves with various amplitudes, it is difficult to decide whether the large activity is caused by a few large-amplitude waves or many small-amplitude waves. In this paper, the Kelvin wave cases and amplitudes at each grid are understood using the extracted Kelvin wave methodology described in section 2.

[18] Figure 3b shows the distribution of total cases for Kelvin waves summed up in each 15° grid for 45 years. The numbers are found by counting cases of Kelvin wave

signals as the easterly maxima seen in Figure 2. The longitude-height distribution of the case numbers seems similar to that of the Kelvin wave activity in Figure 3a; the numbers of Kelvin wave cases (hereafter often called "case number" for simplicity) are large in the eastern hemisphere centered around $60°E-90°E$ at 100 hPa and above, and in the western hemisphere around $120°W$ at $150-250$ hPa.

[19] Figure 3c shows a longitude-height cross section of mean squared amplitude for Kelvin waves selected with the easterly thresholds. Because the amplitude field is noisy, $12.5°$ grid running mean for smoothing in the longitudinal direction is applied. The maximum difference in the mean squared amplitudes is only about 10 m^2 s^{-2} in the region between 200 and 100 hPa. It corresponds to differences of about 3 m s^{-1} in the absolute amplitude. The distribution of
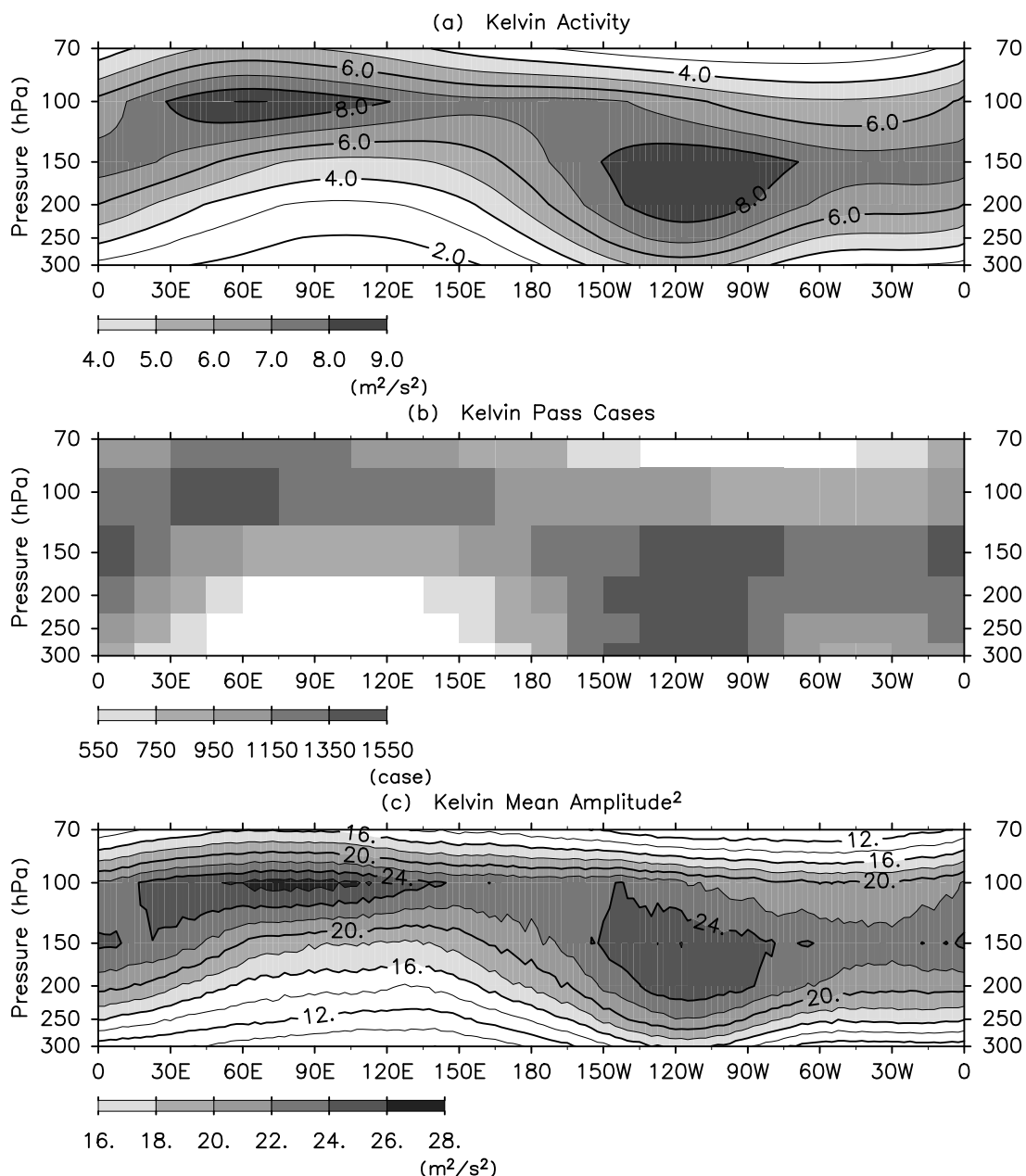
Figure 3. Longitude-height sections of the annual mean for Kelvin waves (a) activity, (b) total cases, and (c) squared amplitudes of zonal wind averaged over latitudes 5°S − 5°S from the ERA-40 reanalysis data.

the mean squared amplitude (Figure 3c) is consistent with the discussion by SS08. We suggest that the wave amplitudes could preferentially increase in the easterly region because of wave distortion in the eastern hemisphere at 100 hPa as the following: Kelvin waves in the easterly region are able to propagate vertically without damping and reach around the tropopause. Then, because of sudden increase in the Brunt-Väisälä frequency N, the Kelvin wave amplitude can increase [cf. *Shiotani and Horinouchi*, 1993]. In the westerly region at 200 hPa wave distortion is possibly due to the high intrinsic wave speed. The climatological background zonal wind in the upper troposphere was easterly in the eastern hemisphere and westerly in the western hemisphere throughout the year.

[20] The Kelvin activity (Figure 3a) is related to the value of the case number (Figure 3b) multiplied by the mean squared amplitude (Figure 3c); however, the waves are selected with the easterly threshold in Figures 3b and 3c. Generally the activity would be affected similarly by both the case number and the mean squared amplitude, because the distributions of all these variables resemble each other closely except for some differences in the details. (For instance, the maximum region is at 100 hPa at 30°E−75°E for the case number but at 60°E−120°E for the mean squared amplitude. This suggests that the Kelvin waves have large amplitudes around 75°E−120°E at 100 hPa; it is consistent that rapid transitions in the zonal wind at 100 hPa occur at 90°E−120°E relative to the amplified Kelvin waves
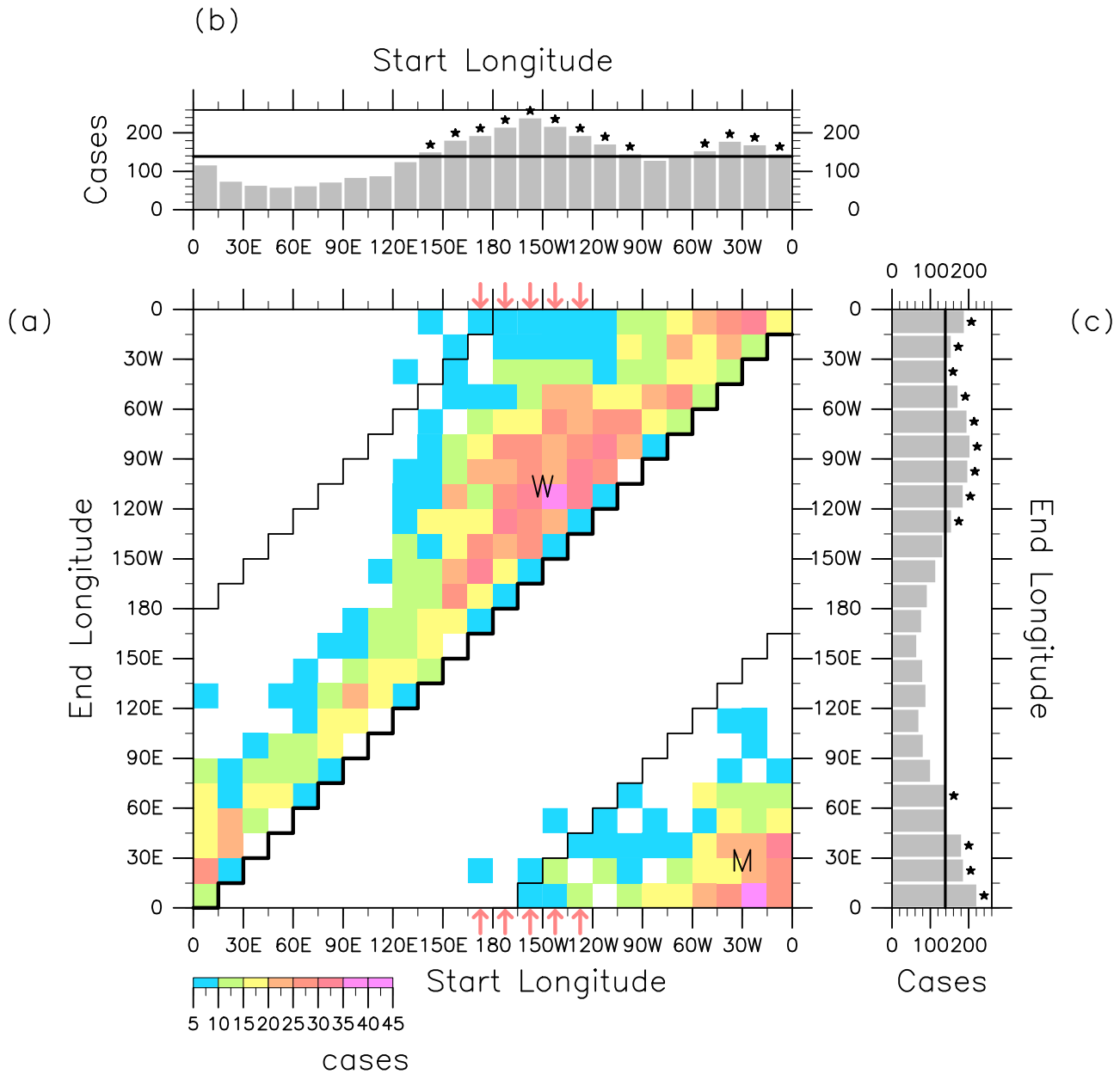
Figure 4. The frequency distributions of (a) appearance-disappearance longitudes, (b) appearance longitudes, and (c) disappearance longitudes for Kelvin waves in the zonal wind at 200 hPa. In Figure 4a, stair-shaped lines show the appearance points (thick line) and the 180° distance from the appearances (thin lines). The letter W means the region around the western hemisphere; the letter M means the middle region (see details in the text). The red arrows represent the regions shown in Figures 6 and 8. In Figures 4b and 4c, stars show the regions above the average, which is indicated by lines (138 cases per 15°).

reported by *Nishi et al.* [2007].) However, because of the general similarities among the three variables, henceforth we will use the case number as an index of Kelvin wave activity.

[21] Though Figure 3b shows the regions of Kelvin wave passage, it does not show where each wave appeared and disappeared. Figure 4a represents the disappearance locations of Kelvin waves relative to the appearance longitudes at 200 hPa, as well as information about where the Kelvin waves pass (Figure 3b). Stair-shaped lines show the appearance points (one thick line) and the 180° distance from the appearances (two thin lines).The characteristic variability of

Kelvin waves in features such as appearance and disappearance region and propagating distance is also shown. Incidentally, fewer than ten cases of Kelvin waves propagating around the globe occur in each field at 200 and 100 hPa (not shown). In Figure 4a, the Kelvin waves are concentrated in two regions. One region, labeled W, is located in the western hemisphere, where the waves appear around 150°E−90°W and disappear around 180°−45°W. Note that Kelvin waves in case W propagate about 80° on the average. In the other, labeled M, the waves appear around 75°W−0°W and disappear around 60°W−45°E. Cases W and M correspond to the regions around 120°W and 0°W,
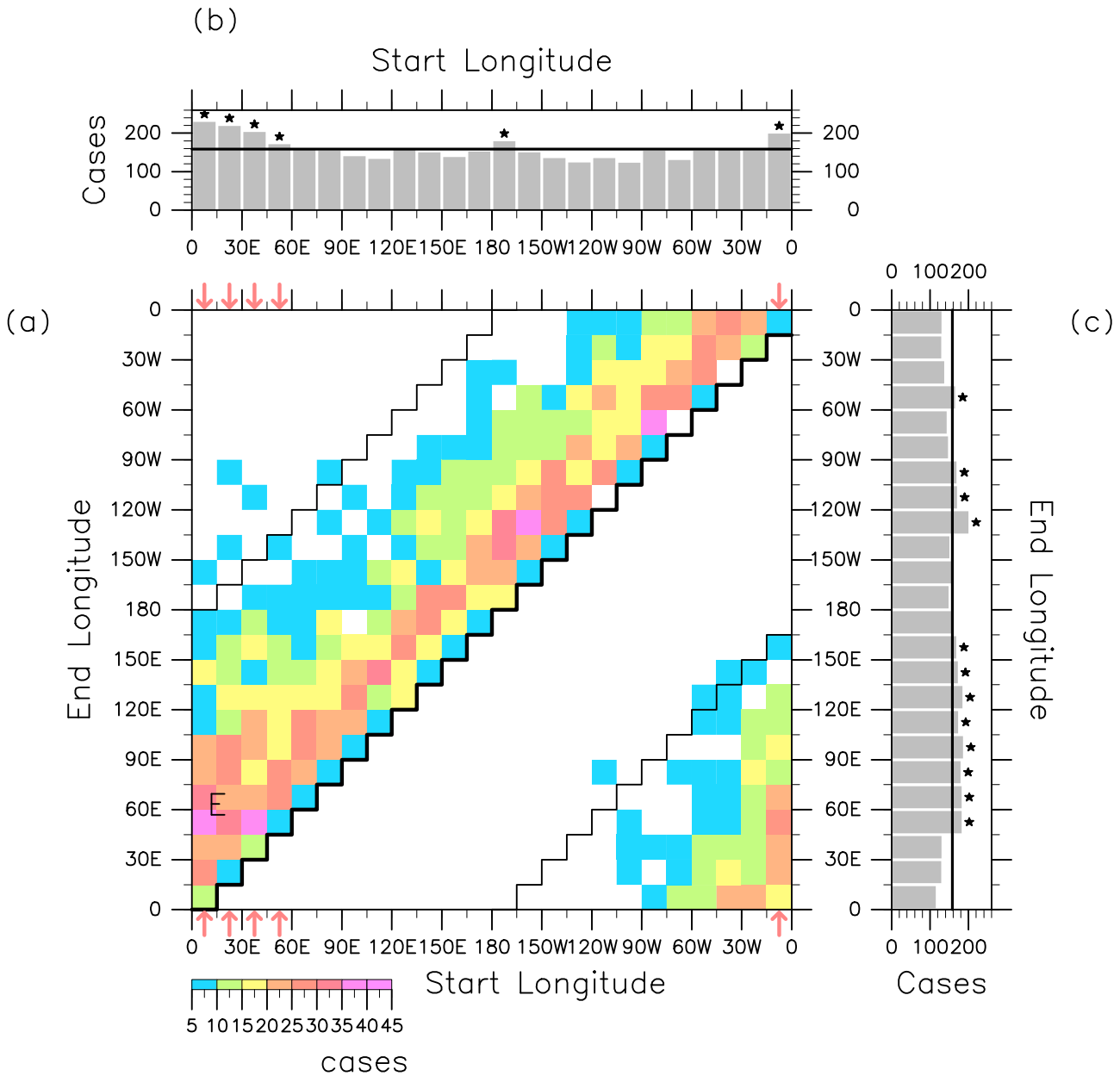
Figure 5. Same as Figure 4 except at 100 hPa. In Figure 5a, the letter E means the region around the eastern hemisphere (see details in the text). The red arrows represent the regions shown in Figures 7 and 9. In Figures 5b and 5c, stars show regions above the average, which are indicated by lines (158 cases per 15°).

respectively, where the Kelvin wave case numbers are large in Figure 3b.

[22] Most of the Kelvin waves show a range from appearance to disappearance of about 90° (six boxes) in longitude at 200 hPa. Kelvin waves appearing east of 120°E propagate relatively long distances (about 80° on the average); furthermore, some Kelvin waves propagate near 180°.

[23] Figure 4b shows histograms of the appearance longitudes for the Kelvin waves. The height of a bar corresponds to the total case number summed up about the disappearance longitudes each appearance longitude in Figure 4a. The total number of appearances at 200 hPa is 3331 cases, and the average is 138 cases per 15° (the

horizontal line). Stars represent high-frequency regions above the average. Two appearance regions are found; one is centered on 165°W corresponding to case W. West of case W is the convective region from the Indian Ocean to the western Pacific shown in Figure 2. Another appearance region is centered on 30°W corresponding to case M. The area west of the region centered on 30°W is also convectively active over the South American continent, as seen in Figure 2. Figure 4c shows histograms of the disappearance longitudes. Two peaks are found; one centered on 90°W corresponds to case W, and another centered on 0°W is related to case M.

[24] Figure 5 is the same as Figure 4 but for Kelvin waves at 100 hPa. In Figure 5a, the highest-frequency region,

labeled E, is centered on the eastern hemisphere where appearances occur around $15°W-60°E$ and disappearances occur around $15°E-120°E$. The appearance and disappearance regions in case E are located about $30°$ east of those in case M. Case E corresponds to the region around $60°E-90°E$ where the case number is large in Figure 3b. Starting from appearance longitudes, most Kelvin waves at 100 hPa propagate about $45°$ distances (three boxes) in the horizontal component. In case E, Kelvin waves propagate about $80°$ on the average and some Kelvin waves reach $180°$ from the appearance points.

[25] Figure 5b shows histograms of the appearance longitudes for Kelvin waves at 100 hPa. The total number of appearances at 100 hPa is 3801, and the average is 158 cases per $15°$ (the horizontal line). All bar heights of the appearance numbers at 100 hPa are generally closer to each other than those at 200 hPa in Figure 4b. However, the peak at 100 hPa is clearly observed around $15°W-15°E$, corresponding to the case E region.

[26] Figure 5c shows histograms of the disappearance longitudes for Kelvin waves at 100 hPa. Though the peak of the disappearance longitudes at 100 hPa is not more remarkable than that at 200 hPa in Figure 4c, Kelvin waves disappear frequently in the two regions around $45°E-165°E$ (corresponding to case E) and around $120°W$.

[27] Figures 4 and 5 clearly indicated that cases W and E are typical examples for Kelvin waves at 200 and 100 hPa, respectively. In section 3.2, composite analysis is applied to further investigate the mean Kelvin wave characteristics at both levels and the relationship between Kelvin waves and dynamical fields or convections.

3.2. Composite Lifecycles of Kelvin Waves

[28] Kelvin waves for zonal wind anomalies in the upper troposphere and around the tropopause are related to the background zonal winds and convective activity. The lifecycle and effective conditions for Kelvin waves are analyzed with a composite method referring to the appearance points crossing the threshold for the easterly wind component ("S" in Figure 2; see details in section 2). From the results in section 3.1, cases W and E are chosen as typical examples for Kelvin waves at 200 and 100 hPa, respectively; we have defined Kelvin waves appearing around $165°E-122.5°W$ at 200 hPa as case W, and those appearing around $15°W-57.5°E$ at 100 hPa as case E. Furthermore, the composite Kelvin waves extracted from these specific longitudes could be used to investigate the approximate longitudinal variabilities. Here, the signals of the composite Kelvin waves are described in the zonal wind component with the anomaly ($[U]'$) from 31 day mean ($[U]_t$) at each grid: $[U]' = [U] - [U]_t$, where the square brackets indicate the latitudinal mean between $5°S$ and $5°N$. Noted that spatial and temporal filters such as that used in Figure 2 are not applied to the composite fields; that is, here the filter is used only to locate the appearance points.

[29] Case W is composed of Kelvin waves whose signals first appear at longitudes between $165°W$ and $122.5°W$ at 200 hPa over the central Pacific. Figure 6 shows relative longitude-time diagrams of zonal wind anomaly ($[U]'$) at 100 hPa (Figure 6a) and 200 hPa (Figure 6b), the OLR anomaly ($[OLR]'$) and total OLR ($[OLR]$) below 222 W m^{-2}, (middle) the 31 day mean zonal wind at 200 hPa ($[U]_t$), and

(bottom) the 31 day mean OLR ($[OLR]_t$). A positive (negative) time lag denotes days after (before) the day of the Kelvin wave's ($[U]'$) appearance in longitude between $165°W$ and $122.5°W$ at 200 hPa. A visual inspection indicates that the composite Kelvin wave has the prevailing zonal wave numbers $1-3$ estimated roughly by the longitudes of zero-to-zero or peak-to-peak for wind anomalies in day 0.

[30] In Figure 6b the negative zonal wind anomaly is found around the referred point (in $0°$ relative longitude, lag day 0) and propagates eastward to the point at $+60°$ at day 5 with an averaged phase speed of about 15 m s^{-1} through the westerly basic wind. After day 7, the signal still continuing from the east of $+110°$ suggests that some Kelvin waves included in case W could propagate roughly a halfway around the globe; this is consistent with the feature seen in Figure 4a. In addition, 10% of case W propagates over $+165°$ (not shown). The largest Kelvin wave amplitude over the lifetime is about 4.0 m s^{-1} in days 2 and 3 around $+30°$, where the strongest westerly mean wind blows (middle).

[31] In Figure 6, two convective regions are found and specified by their longitudes (bottom): they correspond to the Indian Ocean and western Pacific (from $-135°$ to $-15°$ in relative longitude) and South America (from $+80°$ to $+120°$). The lowest $[OLR]_t$ is about 222 W m^{-2} at $-75°$. Of the two, the convective region regarded as the Indian Ocean and western Pacific is active around $-75°$ from days -10 to $+5$ for the total OLR ($[OLR]$) below 222 W m^{-2} where the Kelvin wave signals ($[U]'$ at 200 hPa and $[OLR]'$) in case W appear. The Kelvin wave amplitude decreases around the convective region over South America (from $+80°$ to $+120°$), but then the signal still continues with a higher phase speed than before (Figure 6b).

[32] Around day -2 the signal in the OLR propagating eastward is out-of-phase and precedes by about 3 days the easterly wind at 200 hPa. This suggests that some Kelvin waves included in the composite case W propagate eastward together with convections for a few days. The eastward moving convection ($[OLR]'$) appear over quasi-stationary convections around $-75°$. The cloud tops of deep convection seem to be near 200 hPa because the zonal divergence and the negative OLR anomaly almost agree with each other. Hereafter, a Kelvin wave that propagates together with convection is often called a convectively coupled Kelvin wave [cf. *Wheeler et al.*, 2000]. The longitudes are consistent with the result of *Kiladis et al.* [2009] which shows variabilities of eastward moving convections are large over the central Pacific. Therefore main energy sources for case W are also probably eastward moving convections. Zonal wind anomalies still propagate eastward for a few more days though eastward moving convections disappear around day $+7$ (Figure 6b). At 100 hPa zonal wind anomalies (Figure 6a) propagate farther eastward than at 200 hPa and reach around $-90°$ (equal to $+270°$).

[33] Kelvin wave amplitude increases in day 2 when the largest westerly basic wind occurs, suggesting two possibilities for the relationship between Kelvin wave amplification and the basic wind. One is that the amplification is caused by the westerly wind if the zonal phase speed approaches that of the basic wind. The other is that frequent occurrences of Kelvin waves breaking in the westerly basic wind accelerate the westerly because the basic wind can
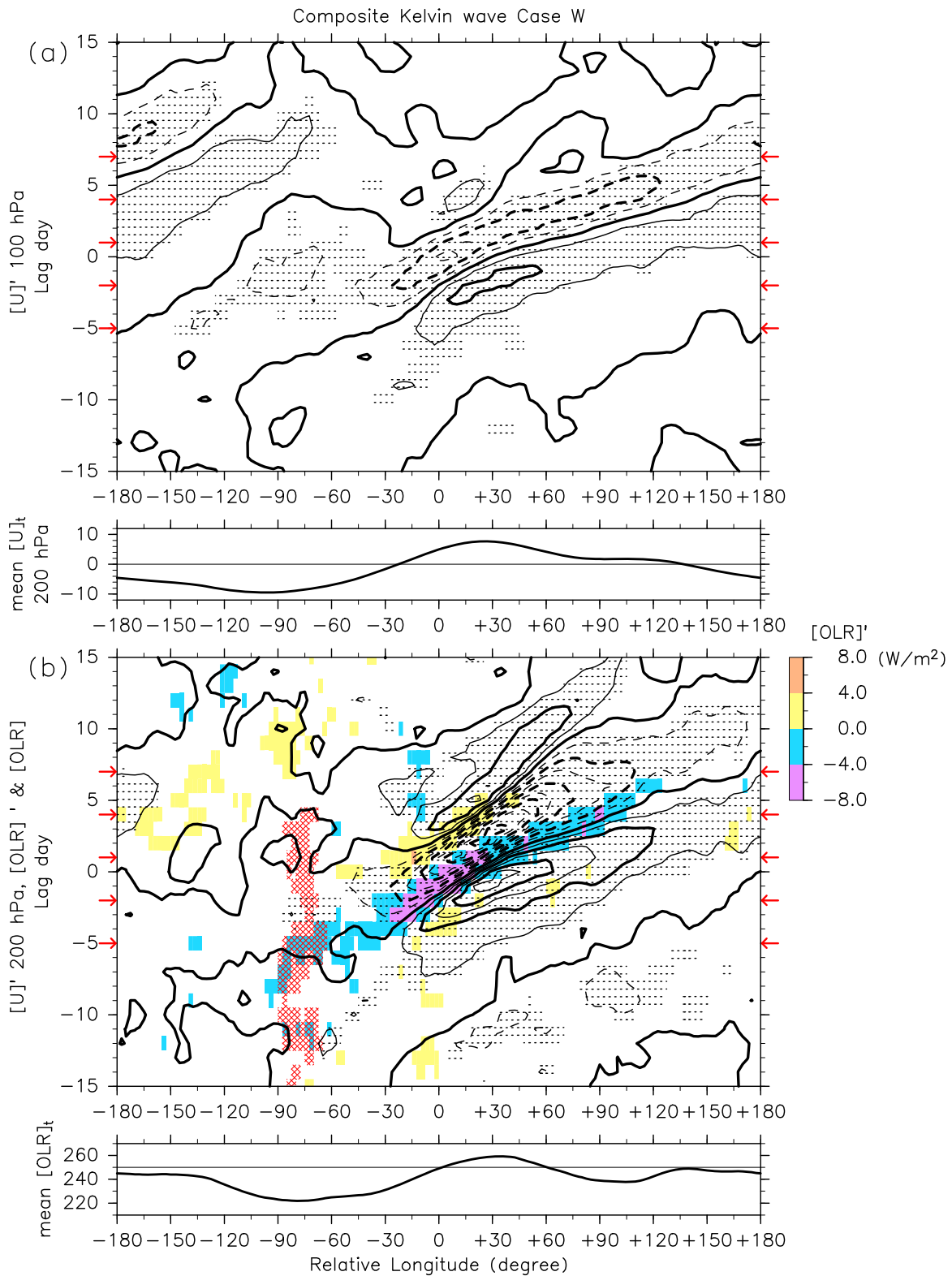
Figure 6. Relative longitude-time diagram of the composite Kelvin wave in case W for the zonal wind anomaly ([U]$'$, contours) at (a) 100 hPa and (b) 200 hPa, OLR anomaly ([OLR]$'$, colors), and total OLR ([OLR], red hatch). Contour interval is 0.5 [m s^{-1}]. Black hatch shows the zonal wind anomaly is locally statistically significant at the 99% level. Only total OLR below 222 [W m^{-2}] is represented. Only OLR anomalies that are locally statistically significant at the 99% level are shown. Red arrows at left and right represent the days described in Figure 8. The 31 day mean of zonal wind ([U]$_t$) at 200 hPa is averaged for total cases; the straight line shows 0 [m s^{-1}]. The 31 day mean of OLR ([OLR]$_t$) is averaged for total cases; the straight line shows 250 [W m^{-2}].
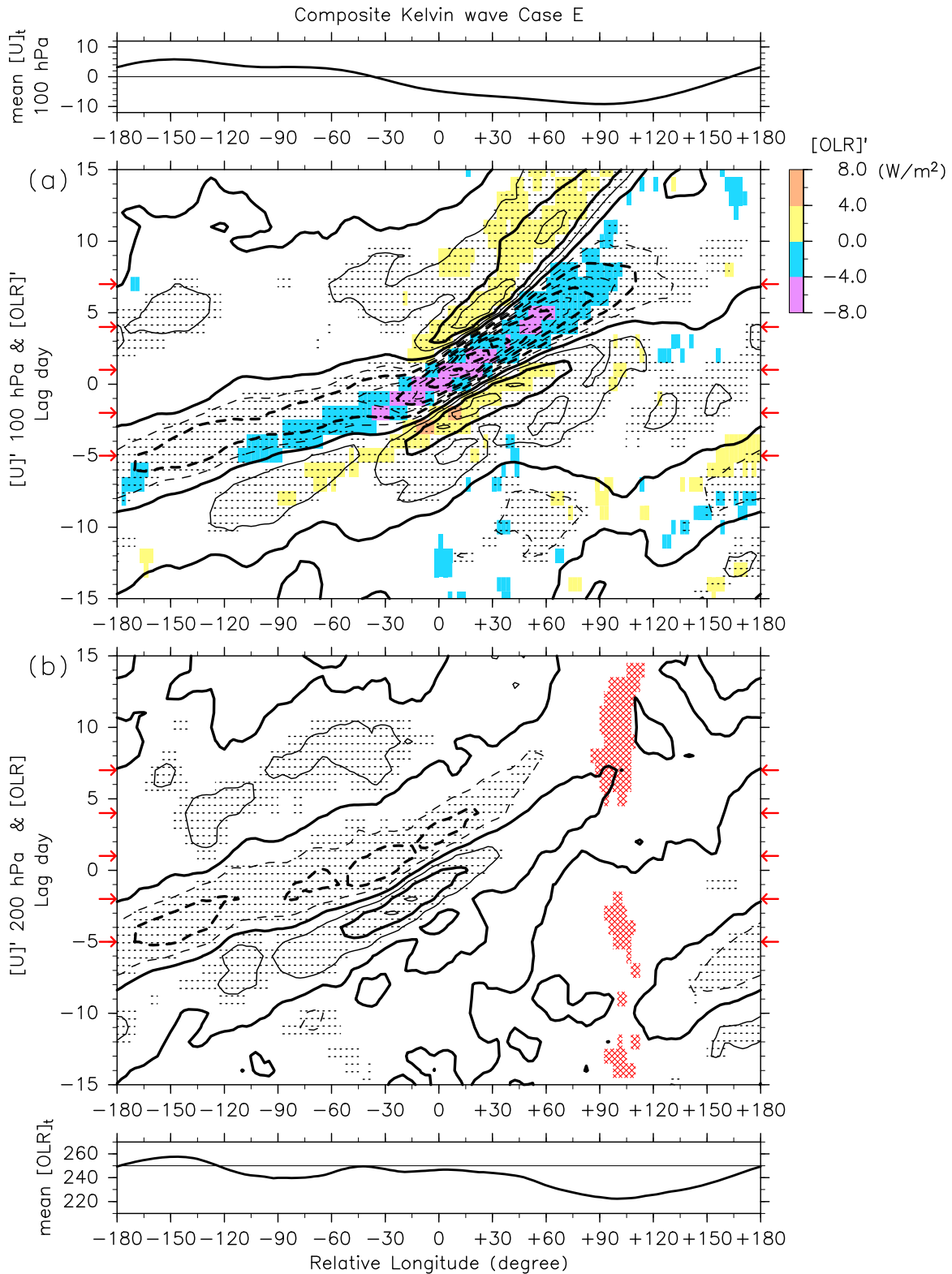
Figure 7. Same as in Figure 6, except in case E for zonal wind anomalies (contours) at (a) 100 hPa and (b) 200 hPa and total OLR below 222.5 [W m^{-2}] (red hatch); the red arrows at left and right represent the days described in Figure 9.

receive westerly momentum from the breaking of eastward-propagating waves. However, we cannot further discuss the possibilities because breaking waves might not be represented in the reanalysis data.

[34] Figure 7 show relative longitude-time diagrams of zonal wind anomaly ([U]′) in the case E at 100 hPa (Figure 7a) and the OLR anomaly ([OLR]′, [U′] at 200 hPa (Figure 7b) and total OLR ([OLR]) below 222.5 W m^{-2},

(upper) the 31 day mean zonal wind at 100 hPa ($[U]_t$) and (bottom) the 31 day mean OLR ($[OLR]_t$). Case E, composed of Kelvin waves whose signals first appear in longitudes between 15°W and 57.5°E at 100 hPa from the eastern Atlantic Ocean to the western Indian Ocean, is selected as a typical example of Kelvin waves around the tropopause region. Two convective regions are confirmed by the longitudinal distribution of the 31 day mean OLR (bottom): they are over South America (around −90° in relative longitude) and the Indian Ocean and western Pacific (from +60° to +115°). The lowest $[OLR]_t$ is about 222.5 W m^{-2} at +100°. In Figure 7a the easterly anomaly for zonal wind around 0° in day 0 propagates eastward, and then reaches a point at +90° in day 8 in a convectively active area characterized by total OLR below 222.5 W m^{-2} and strong easterly winds ($\sim$10 m s^{-1}). Waves passing through the easterly basic wind have a phase speed of about 15 m s^{-1} on average. The Kelvin wave amplitude is largest (about 4.0 m s^{-1}) around +30° on day 2. From west of the convection over South America, the Kelvin wave signal is continuously traced as far as around −180° on about day −5 with a phase speed of $\sim$35 m s^{-1} through the westerly basic wind.

[35] The OLR anomaly propagates eastward almost in phase with the easterly wind anomaly when they pass through the active convective regions over South America and the Indian Ocean and western Pacific Ocean. This suggests that some Kelvin waves in case E are also convectively coupled similar to those in case W at 200 hPa; however, here the OLR anomalies are smaller than the values obtained through the analysis by *Wheeler et al.* [2000] on Kelvin wave signals in the OLR (compare their Figure 4) partly because our composites would be set on the basis of easterly wind. During the easterly anomaly associated with the OLR anomaly, with respect to the phase relationship between these two variables, case E at 100 hPa differs from case W at 200 hPa; the convectively coupled Kelvin wave has a vertical structure in which the phase for zonal wind anomaly tilts toward the east with height [e.g., *Wheeler et al.*, 2000; *Straub and Kiladis*, 2003]. The vertical structures of the Kelvin waves will be represented in Figures 8 and 9. In case E convective suppressed signals ($[OLR]' > 0$) and westerly wind anomalies at 100 hPa propagate eastward after negative convective anomalies and easterly wind anomalies are disappear around +90° in day +10 (Figure 7a). At 200 hPa positive and negative zonal wind anomalies disappear around day = +10 (Figure 7b).

[36] Next, the vertical structure of the zonal wind anomalies ($[U]'$) and the temperature anomalies ($[T]'$) in cases W and E are presented to confirm whether the cases have the structure of theoretical pure free Kelvin waves [e.g., *Andrews et al.*, 1987] and the amplitude of temperature field disturbances at each height as time goes by. Investigating the temperature fluctuations in the TTL and upper troposphere is particularly important because they act directly to dehydrate air entering the lower stratosphere.

[37] Figure 8 shows the relative longitude-height distribution of the zonal wind and temperature anomalies for days −5, −2, 1, 4, and 7 in case W, corresponding to the days marked by red arrows in Figure 6. At day −5, a cold anomaly in the lower troposphere and a warm anomaly around 400 hPa (Figure 8) are found near the active convection around −90° (Figure 6), but the Kelvin wave

is not clear in the zonal wind field. In day −2, zonal divergence exists in the upper and middle troposphere centering around 200 hPa on 0°, and weak convergence appears in the lower troposphere. This vertical system such as a cell moves eastward. After day −2, the temperature anomalies show 0 K borders for anomalies sloping westward with height from 850 hPa to about 300 hPa, and sharply eastward at greater heights. Hereafter, vertical structure that tilts eastward (westward) with increasing (decreasing) height from the middle troposphere $\sim$300 hPa to the lower troposphere (lower stratosphere), accompanied by a zonal wind anomaly that is delayed about a quarter wavelength from the temperature anomaly, is called a boomerang-like vertical structure. The longitudes of convection and zonal divergence at 200 hPa (Figure 6) located slightly in front of the elbow of this boomerang-like vertical structure for the warm anomaly at 300 hPa in day 1 (Figure 8) are consistent with the vertical structure of a convectively coupled Kelvin wave described by *Wheeler et al.* [2000]. This phase relationship between the warm anomaly at the corner and the zonal wind anomaly around 200 hPa loosens in day 7 (Figure 8) because of unclear accompanying convections (Figure 6). On day 7, the easterly anomaly centered on the upper troposphere reaches around +80°, which is regarded as being near the convective region over South America in Figure 6. The temperature anomaly is weak throughout days −2 to 7, but above 100 hPa the temperature anomaly is somewhat large.

[38] Figure 9 shows the same information as Figure 8 but for case E. The zonal wind and temperature anomalies are large at 100 and 70 hPa. On days 1 and 4, the easterly wind anomaly is large at 100 hPa around +30°, which is regarded as the region between the African continent and the Indian Ocean and western Pacific Ocean seen in Figure 7. In general, the temperature anomaly is larger than in case W. Above the upper troposphere, the phase for temperature anomaly precedes that for zonal wind anomaly about 90°, with both anomalies tilting toward the east, agrees with the Kelvin wave vertical structure predicted theoretically for upward propagating as the free mode [e.g., *Andrews et al.*, 1987]. The boomerang-like vertical structure for the temperature anomaly is also clear in days −2, 1, and 4, while the Kelvin wave propagates eastward with the convections (Figure 7). On day 7, the Kelvin wave amplitude decreases after it rushes into the strong easterly and convective region around +115° between the Indian Ocean and the western Pacific, as found in Figure 7.

[39] The connection between case E for an example at 100 hPa and case W at 200 hPa will be discussed in terms of longitudinal and temporal locations. Some waves in case W would be regarded as being in case E if they could propagate eastward and upward to the 100 hPa level in the eastern hemisphere. In case W, the relative longitude of South America is around +100° in Figure 6, where a Kelvin wave for the easterly anomaly tilting eastward with increasing height has been found on day 7 in Figure 8. This structure of temperature perturbation is consistent with a vertically propagating Kelvin wave [e.g., *Andrews et al.*, 1987]. In case E, the convective region over South America has already been regarded as the region around the relative longitude of −90° in Figure 7, where the phase of the easterly anomaly also tilts eastward with increasing height
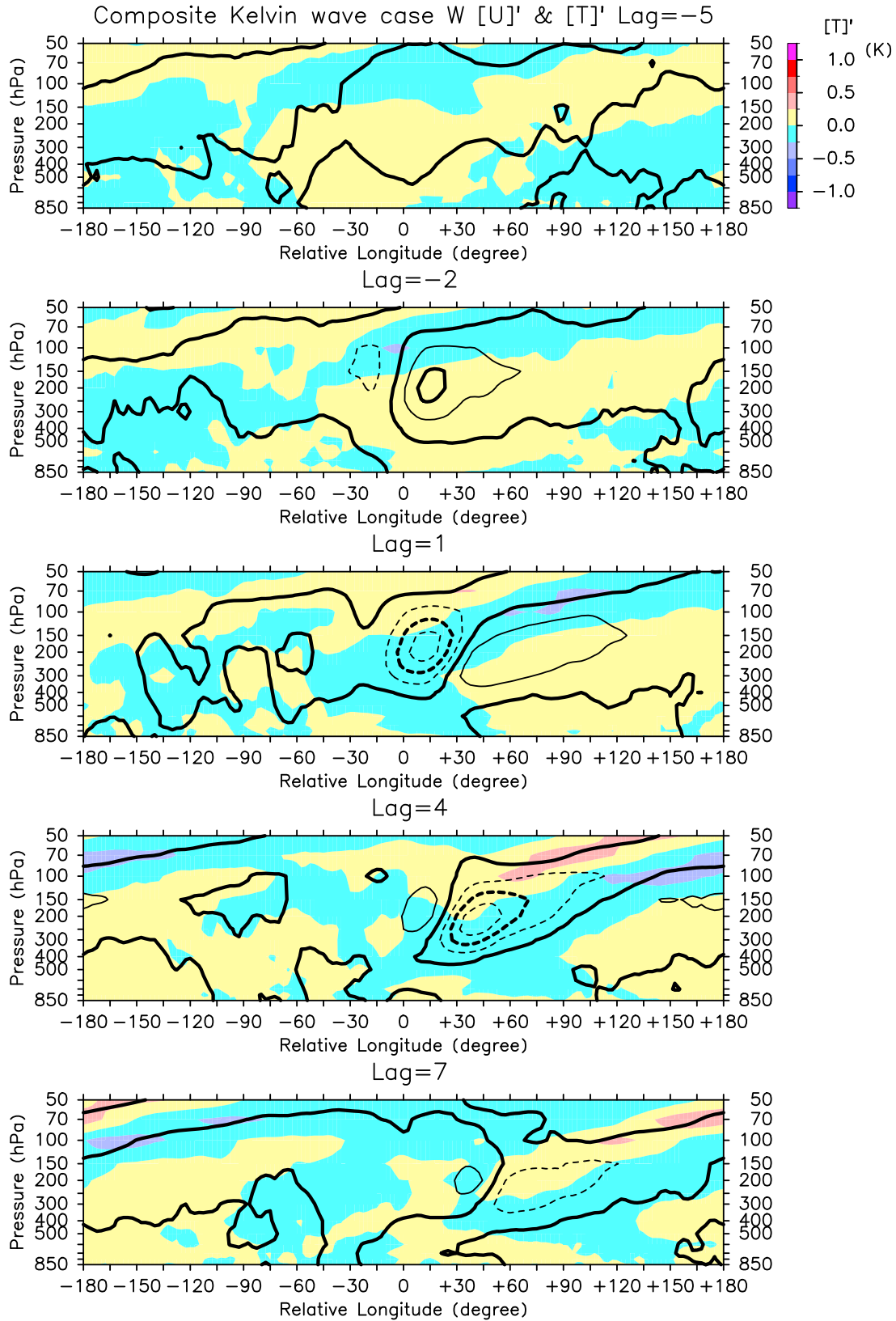
Figure 8. Relative longitude-height cross sections of the zonal wind anomalies ([U]′; contours) and temperature anomalies ([T]′; shading) for the composite Kelvin wave in case W for day −5, day −2, day +1, day +4, and day +7. Contour interval is 1.0 [m s⁻¹].
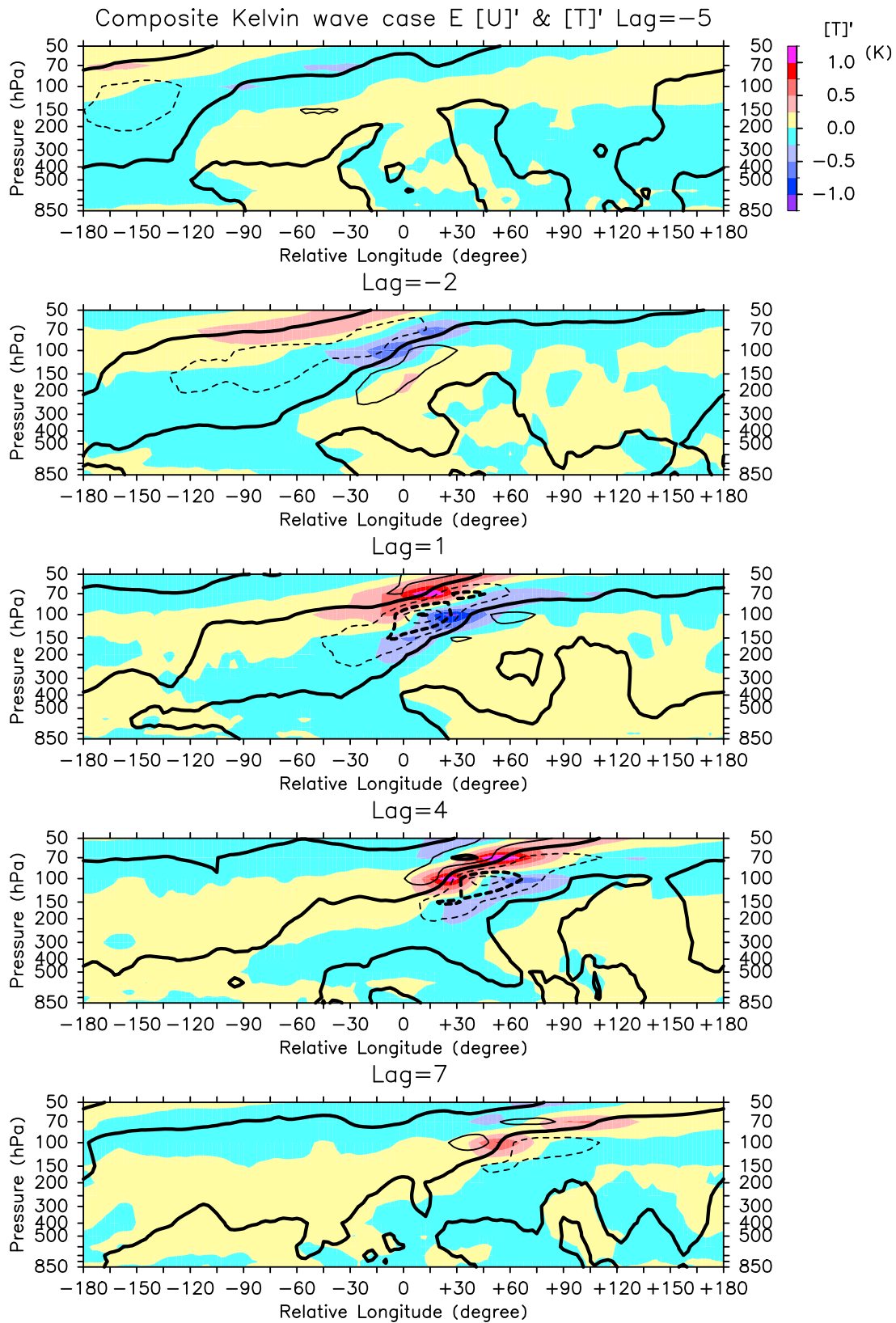
Figure 9. Same as in Figure 8, except for the composite Kelvin waves in case E.

from near the 500 hPa level in Figure 9. On day −5, three days before the above, the easterly anomaly is centered at 150 hPa in the upper troposphere around −150° in case E. Therefore, it could be suggested that some of the Kelvin waves first found in the western hemisphere at 200 hPa (called case W) propagate upward and eastward near South America and then reach 100 hPa in the eastern hemisphere (called case E).

4. Summary

[40] Using the ECMWF 40 year reanalysis data for the zonal wind field, we have investigated the characteristic variability and typical lifecycles of Kelvin waves around the tropical tropopause layer (TTL) and upper troposphere. The distributions of Kelvin wave activity, mean squared amplitude, and number of passing cases closely resemble each other. The case number is chosen as an index to Kelvin wave activity.

[41] Kelvin wave disappearance locations related to their appearance longitudes were investigated at 200 hPa in the upper troposphere and at 100 hPa in the TTL. At 200 hPa the Kelvin waves mostly concentrate in a region in the western hemisphere (case W) where the waves appear around 150°E−90°W and disappear around 180°W−45°W. At 100 hPa the highest-frequency region, named case E, is centered on the eastern hemisphere appearing around 15°W−60°E and disappearing around 15°E−120°E. In both cases most Kelvin waves propagate, from appearance to disappearance, as far as about 80° in longitude on average; however, some propagate nearly 180° from the appearance longitude. At 100 hPa, most Kelvin waves propagate about 45°.

[42] From the composite analysis, Kelvin waves appearing around 165°E−122.5°W at 200 hPa seem to appear over deep convections between the Indian Ocean and the western Pacific. These waves propagate eastward through the mean westerly wind and decrease in amplitude. Weak signals continue to propagate with acceleration over South America. Some Kelvin waves propagate eastward together with convections for a few days. Cloud tops of the eastward-propagating convections seem to be near 200 hPa.

[43] At 100 hPa, Kelvin waves appearing around 15°W−57.5°E seem to appear over deep convection around South America, and the signals propagate eastward into another convective region located over the Indian Ocean and western Pacific Ocean. West of South America, the signals are traced upstream; some waves found at 200 hPa could propagate up to the 100 hPa level. The OLR and easterly wind anomalies propagate eastward in phase around the appearance region: convectively coupled Kelvin waves are included in these waves found at 100 hPa over the Indian Ocean and western Pacific.

[44] This paper clearly shows the characteristic variability around the TTL and the typical lifecycle of the Kelvin waves at 100 hPa in the eastern hemisphere and 200 hPa in the western hemisphere. In both hemispheres the composite Kelvin waves include so-called convectively coupled Kelvin waves. The dynamical structure of Kelvin waves in relation to the strength and weakness of convective coupling would be another noteworthy topic to investigate.

References

Alexander, S. P., T. Tsuda, Y. Kawatani, and M. Takahashi (2008), Global distribution of atmospheric waves in the equatorial upper troposphere and lower stratosphere: COSMIC observations of wave mean flow interactions, *J. Geophys. Res.*, 113, D24115, doi:10.1029/2008JD010039.
Andrews, D. G., J. R. Holton, and C. B. Leovy (1987), *Middle Atmosphere Dynamics*, 489 pp., Academic, San Diego, Calif.
Baldwin, M., et al. (2001), The quasi-biennial oscillation, *Rev. Geophys.*, 39, 179−229, doi:10.1029/1999RG000073.
Boehm, M. T., and J. Verlinde (2000), Stratospheric influence on upper tropospheric tropical cirrus, *Geophys. Res. Lett.*, 27, 3209−3212, doi:10.1029/2000GL011678.
Ern, M., P. Preusse, M. Krebsbach, M. G. Mlynezak, and J. M. Russell III (2008), Equatorial wave analysis from SABER and ECMWF temperatures, *Atmos. Chem. Phys.*, 8, 845−869.
Fujiwara, M., K. Kita, and T. Ogawa (1998), Stratosphere-troposphere exchange of ozone associated with the equatorial Kelvin wave as observed with ozonesondes and rawinsondes, *J. Geophys. Res.*, 103, 19,103−19,182, doi:10.1029/98JD01419.
Fujiwara, M., F. Hasebe, M. Shiotani, N. Nishi, H. Vömel, and S. J. Oltmans (2001), Water vapor control at the tropopause by equatorial Kelvin waves observed over the Galápagos, *Geophys. Res. Lett.*, 28, 3143−3146, doi:10.1029/2001GL013310.
Holton, J. R. (1972), Waves in the equatorial stratosphere generated by tropospheric heat sources, *J. Atmos. Sci.*, 29, 368−375, doi:10.1175/1520-0469(1972)029<0368:WITESG>2.0.CO;2.
Immler, F., K. Kruger, M. Fujiwara, G. Verver, M. Rex, and O. Schrems (2008), Correlation between equatorial Kelvin waves and the occurrence of extremely thin ice clouds at the tropical tropopause, *Atmos. Chem. Phys.*, 8, 4019−4026.
Kiladis, G. N., M. C. Wheeler, P. T. Haertel, K. H. Straub, and P. E. Roundy (2009), Convectively coupled equatorial waves, *Rev. Geophys.*, 47, RG2003, doi:10.1029/2008RG000266.
Nishi, N., J. Suzuki, A. Hamada, and M. Shiotani (2007), Rapid transitions in zonal wind around the tropical tropopause and their relation to the amplified equatorial Kelvin waves, *Sci. Online Lett. Atmos.*, 3, 13−16, doi:10.2151/sola.2007-004.
Peter, T., et al. (2003), Ultrathin tropical tropopause clouds (UTTCs): I. Cloud morphology and occurrence, *Atmos. Chem. Phys.*, 3, 1083−1091.
Ryu, J.-H., S. Lee, and S.-W. Son (2008), Vertically propagating Kelvin waves and tropical tropopause variability, *J. Atmos. Sci.*, 65, 1817−1837, doi:10.1175/2007JAS2466.1.
Salby, M. L., and R. R. Garcia (1987), Transient response to localized episodic heating in the tropics. Part I: Excitation and short-time near-field behavior, *J. Atmos. Sci.*, 44, 458−498, doi:10.1175/1520-0469(1987)044<0458:TRTLEH>2.0.CO;2.
Shiotani, M., and T. Horinouchi (1993), Kelvin wave activity and the quasibiennial oscillation in the equatorial lower stratosphere, *J. Meteorol. Soc. Jpn.*, 71, 175−182.
Straub, K. H., and G. N. Kiladis (2002), Observations of a convectively coupled Kelvin wave in the eastern Pacific ITCZ, *J. Atmos. Sci.*, 59, 30−53, doi:10.1175/1520-0469(2002)059<0030:OOACCK>2.0.CO;2.
Straub, K. H., and G. N. Kiladis (2003), The observed structure of convectively coupled Kelvin waves: Comparison with simple models of coupled wave instability, *J. Atmos. Sci.*, 60, 1655−1668, doi:10.1175/1520-0469(2003)060<1655:TOSOCC>2.0.CO;2.
Suzuki, J., and M. Shiotani (2008), Space-time variability of equatorial Kelvin waves and intraseasonal oscillations around the tropical tropopause, *J. Geophys. Res.*, 113, D16110, doi:10.1029/2007JD009456.
Takashima, H., and M. Shiotani (2007), Ozone variation in the tropical tropopause layer as seen from ozonesonde data, *J. Geophys. Res.*, 112, D11123, doi:10.1029/2006JD008322.
Takayabu, Y. N. (1994), Large-scale cloud disturbances associated with equatorial waves, Part I: Spectral features of the cloud disturbances, *J. Meteorol. Soc. Jpn.*, 72, 433−449.
Tsuda, T., Y. Murayama, H. Wiryosumarto, S. W. B. Harijono, and S. Kato (1994), Radiosonde observations of equatorial atmosphere dynamics over Indonesia 1. Equatorial waves and diurnal tides, *J. Geophys. Res.*, 99, 10,491−10,505, doi:10.1029/94JD00355.
Uppala, S. M., et al. (2005), The ERA-40 re-analysis, *Q. J. R. Meteorol. Soc.*, 131, 2961−3012, doi:10.1256/qj.04.176.

Wheeler, M., and G. N. Kiladis (1999), Convectively coupled equatorial waves: Analysis of clouds and temperature in the wave number–frequency domain, *J. Atmos. Sci.*, *56*, 374–399, doi:10.1175/1520-0469(1999)056<0374:CCEWAO>2.0.CO;2.

Wheeler, M., G. N. Kiladis, and P. J. Webster (2000), Large-scale dynamical fields associated with convectively coupled equatorial waves, *J. Atmos. Sci.*, *57*, 613–640, doi:10.1175/1520-0469(2000)057<0613:LSDFAW>2.0.CO;2.

Winker, D. M., and C. R. Trepte (1998), Laminar cirrus observed near the tropical tropopause by LITE, *Geophys. Res. Lett.*, *25*, 3351–3354, doi:10.1029/98GL01292.

————————————

N. Nishi, Graduate School of Science, Kyoto University, Kyoto 606-8502, Japan.

M. Shiotani, Research Institute for Sustainable Humanosphere, Kyoto University, Gokasho, Uji 611-0011, Japan.

J. Suzuki, Research Institute for Global Change, Japan Agency for Marine-Earth Science and Technology, Natsushima 2-15, Yokosuka 237-0061, Japan. (suzukij@jamstec.go.jp)